Variations in the precipitation–runoff relationship of the Weihe River Basin

Aijun Guo, Jianxia Chang, Dengfeng Liu, Yimin Wang, Qiang Huang and Yunyun Li

ABSTRACT

The main goal of this study is to introduce the Archimedean copulas, which overcome the low accuracy and subjective nature of the traditional double mass curve method, to investigate the precipitation–runoff relationship (PRR) and detect change points in the Weihe River Basin (WRB). With the construction of a joint distribution between precipitation and runoff by the Archimedean copulas, a statistical variable considering the distribution parameter was estimated to judge the change point of the PRR. The results show that: (1) annual precipitation and runoff present decreasing trends that are significant and insignificant, respectively, at the 95% significance level, while annual potential evapotranspiration (PET) increases slightly; (2) change points of the PRR occurred in 1971 and 1994; (3) the annual runoff changed more dramatically than precipitation during the periods from 1972 to 1994 and 1995 to 2010 compared with 1960–1971, which indicates that in addition to precipitation, there are some other non-precipitation factors that are responsible for the change in the PRR; and (4) the contributions to runoff from human activities declined from 1972 to 1994 (84.15%) and 1995 to 2010 (57.16%). These results suggest that human activities (e.g., irrigation, reservoirs, water-and-soil conservation) were the primary driving forces leading to changes in the PRR in the WRB.

Key words | Archimedean copulas, climate change, human activities, precipitation–runoff relationship, Weihe River Basin

Aijun Guo
Jianxia Chang (corresponding author)
Dengfeng Liu
Yimin Wang
Qiang Huang
Yunyun Li
State Key Laboratory Base of Eco-hydraulic Engineering in Arid Area,
Xi'an University of Technology,
Xi'an 710048,
China
E-mail: *chxiang@xaut.edu.cn*

INTRODUCTION

The precipitation–runoff relationship (PRR) is an important issue in engineering hydrology, water resource planning and management, and watershed system evolution (Areerachakul & Junsawang 2014; Nourani *et al.* 2015; Wang *et al.* 2015). It is widely known that the global environment has undergone a drastic change over the past century, increasing the complexity of the hydrological cycle in many regions (Zhang *et al.* 2011; Rahmani & Zarghami 2015; Rege *et al.* 2015). The PRR has undergone great changes in many regions, and presents challenges for water regulation and management. Hence, an in-depth understanding of the PRR (i.e., when, how, and why the PRR changes) is an important issue and should be addressed.

The focus of studies involving the PRR should be when it changes (i.e., detecting the change point(s) of the PRR); however, studies on the change point(s) of the PRR are still lacking. The double mass curve method, which is a simple and practical method, is the most widely used method for testing the long-term evolution tendencies between hydrological and meteorological elements. However, when utilizing the double mass curve method, there is considerable subjectivity in estimating the change point by visual assessment and the inherent variability in hydrologic data (Searcy *et al.* 1960). Some researchers have also applied the cross wavelet spectrum and wavelet transform coherence to study the PRR (Labat *et al.* 2001; Charlier

doi: 10.2166/nh.2016.032

et al. 2015); however, the cross wavelet spectrum and wavelet transform coherence were better for analyzing the periodic properties of two time series and failed to identify the change point(s) of the relationship between the two series. Wang et al. (2015) applied the correlation coefficient to detect the change point of the PRR. Although this method was able to estimate a linear relationship, it was unable to handle non-linear relationships (such as the PRR) because it ignores the structure of the dependence. To avoid these restrictions of the methods mentioned above, the Archimedean copulas (Huang et al. 2015; Jiang et al. 2015a) were introduced to resolve the structure change of the PRR in this study. This method was chosen primarily because of its ability to accurately catch non-linear and asymmetric correlation characteristics between variables.

There have been a number of studies on changes in precipitation and runoff worldwide. Mwale et al. (2009) found that precipitation variability accounted for some runoff variability; however, on its own, it was insufficient for describing catchment runoff variability in southern Alberta and parts of northwestern Alberta. Yang & Tian (2009) showed that intensive human activities, especially agricultural water use, resulted in significant runoff change points, while they had little impact on precipitation in the Haihe River Basin. Zhang et al. (2011) found that annual precipitation declined more than runoff in the downstream of the Huaihe River. All of these studies indicate that the changes in runoff and precipitation are asynchronous, and that the response of runoff to precipitation varies in response to a changing environment. Partal (2012) showed that variability of both the runoff and the precipitation is generally similar over time, with a noticeable decrease in runoff at all of the stations in the Aegean region of Turkey. Velpuri & Senay (2013) investigated the long-term (1950–2009) trends in precipitation, runoff, and runoff coefficient in major urban watersheds in the United States and showed that most of the stations exhibited a downward trend in precipitation, while nearly half of the stations showed an upward trend in runoff. For the Weihe River Basin (WRB) specifically, many studies have been conducted on this issue (Zhan et al. 2014; Xiong et al. 2014); however, previous studies have mainly focused on the changes in a single hydrological factor (e.g., runoff, precipitation, temperature). In recent years, the response of runoff to climate variability and human activities has also become a focus of research in this region (Du & Shi 2012; Chang et al. 2015; Jiang et al. 2015b). However, there have been few studies regarding the law of water recurrence under the changing environment and the relationships between hydrological variables, such as precipitation and runoff.

The Weihe River is one of the most important industrial and agricultural production zones in China, and has presented a complicated PRR under the changing environment. Furthermore, water issues in this region have had a negative impact on societal and ecosystem development. The main purposes of this paper are to: (1) detect the structure change of the PRR; (2) explore the precipitation and runoff changes over different time scales; and (3) analyze the influence of human activities on the PRR by the climate elasticity method. The methodology used in this study can also provide useful insights for detecting the change points in relationships between other hydrological series. The results of this research provide insights for water resources management and planning departments.

STUDY AREA AND DATASET

Study area

The Weihe River (104–110 °E, 33–37 °N) is the largest tributary of the Yellow River, with a total length of 818 km and drainage area of 134,800 km^2, and lies in the semi-humid and semi-arid transitional zone (Figure 1). It originates from the mountains in the southern Gansu Province and passes through 502 km of Shaanxi Province. It is the primary water supply for 0.93 million hm^2 of fertile fields in the Guanzhong Plain and supports more than 61% of Shaanxi province's population.

The WRB is dominated by semi-arid hydrological characteristics and has a continental monsoon climate (Zuo et al. 2012). The climate is dry and chilly in winter and hot and rainy in summer. The mean annual temperature is 7.8 ~ 13.5 °C, and the maximum and minimum temperatures have been observed in July and January (42.8 °C and −28.1 °C, respectively). The annual precipitation is 634.9 mm, of which approximately 60% falls between June and October. The mean annual natural runoff of the river is 10.4 billion m^3

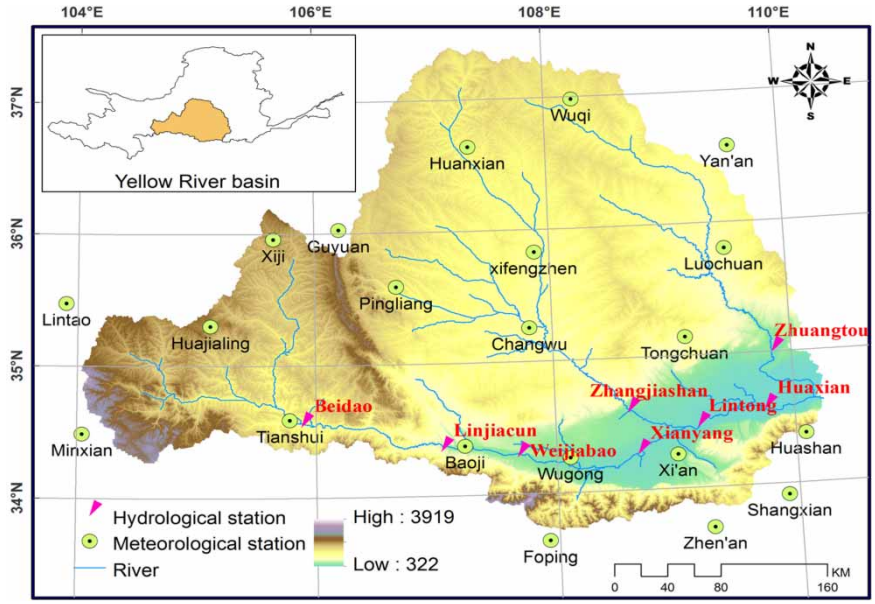

Figure 1 | Locations of hydrological and meteorological stations in the WRB.

and accounts for 17.3% of the Yellow River's total discharge. The seasonal variations in runoff are similar to precipitation. The runoff in July and October accounts for approximately 65% of the mean annual runoff. The annual potential evapotranspiration (PET) is 800–1,200 mm and decreases from north to south. Maximum evaporation occurs in June or July, and evaporation between May and August accounts for 46 ~ 58% of the mean annual evaporation.

During the past 50 years, runoff in the Weihe River has decreased dramatically; in particular, in the late 1990s the average runoff was only 3.60 billion m³ compared to 6.20 billion m³ in the 1950s.

Dataset

Monthly and annual runoff series (1960–2010) from gauging stations throughout the basin, including Huaxian and Zhuangtou, were provided by the hydrology bureau of the Yellow River Conservancy Commission (Figure 1). For this study, we assumed that the sum of runoff from the Huaxian and Zhuangtou stations represented the total runoff generated in the WRB.

The meteorological data (1960–2010) from 21 meteorological stations (Figure 1) inside and outside the WRB, including daily, monthly, and annual precipitation, daily mean temperature, daily maximum temperature, daily minimum temperature, air pressure, relative humidity, wind velocity, and sunshine duration, were provided by the China Meteorological Data Sharing Service System (http://cdc.cma.gov.cn). Daily PET was calculated by the FAO56 Penman–Monteith method using meteorological data (Allen *et al.* 1998). Based on the results from individual stations, the annual precipitation and PET of the whole catchment were calculated by the Thiessen polygon method on the ArcGIS platform. The Thiessen polygon method is a widely used technique and important method to evaluate regional precipitation or PET quantity (Faisal & Gaffar 2012). The first step of this method is to calculate station weights based on the areas of each station. Then the weights are multiplied by the precipitation or PET at the corresponding station to obtain the regional mean precipitation or PET.

METHODOLOGY

FAO56 Penman–Monteith method

The Penman–Monteith method is recommended by the Food and Agriculture Organization (FAO) of the United

Nations and is considered to be the most effective method for estimating PET. The specific calculation formulas used are from Zuo et al. (2012), which can be expressed as:

$$PET = \frac{0.408\Delta(R_n - G) + \gamma \frac{900}{T+273}\mu_2(e_s - e_a)}{\Delta + \gamma(1 + 0.34\mu_2)} \quad (1)$$

where PET is PET (mm/day), Δ is slope of saturated vapour–pressure curve (kPa/°C), Rn is net radiation at the crop surface (MJ/(m^2·day)), G is soil heat flux (MJ/(m^2·day)), γ is psychrometric constant (kPa/°C), T is mean daily air temperature at 2 m height (°C), μ_2 is wind speed at 2 m height (m/s), e_s is saturation vapour pressure (kPa), e_a is actual vapour pressure (kPa) and $e_s - e_a$ is saturated vapour pressure deficit (kPa).

The Archimedean copulas

For the joint function, given that we have n vectors of observations that can be notated (x_1, y_1), (x_1, y_1) …… (x_n, y_n), the marginal distributions are $F(x)$ and $G(y)$, respectively. If $F(x)$ and $G(y)$ are continuous, then there is a unique two-dimensional joint function $C_\theta(u, v)$, which is expressed as:

$$H(x, y) = C_\theta(F(x), G(y)),\ \forall x, y \quad (2)$$

where $C_\theta(u, v)$ is the copula function, θ is the parameter to be estimated, and u and v are the marginal distributions for $F(x)$ and $G(y)$, respectively.

In hydrology research, Archimedean copulas are popular because of the explicit functional forms, including the Clayton, Frank, and Gumbel–Hougaard copulas, are flexible and allow for differences in tail behavior. As shown by Genest & MacKay (1986), the relationship between the Kendall correlation coefficient τ and the generator of Archimedean copulas ($\varphi(t)$) is:

$$\tau = 1 + 4\int_0^1 \frac{\varphi(t)}{\varphi'(t)}dt \quad (3)$$

The expression of the Kendall correlation coefficient τ and the parameter θ of the three copula functions are shown in Table 1.

To build a model of joint distribution on runoff and precipitation, the first step is to obtain an appropriate marginal distribution. In this paper, the generalized extreme value distribution (Gev), logarithmic normal distribution (Logn), and gamma distribution (Gam) were applied to fit the marginal distribution. To identify an appropriate marginal distribution, we utilized root mean square error (RMSE) and Akaike information criteria (AIC) to evaluate distributions.

The RMSE (Equation (4)) is expressed as:

$$RMSE = \sqrt{MSE} = \sqrt{\frac{1}{n}\sum_{i=1}^{n}[x_c(i) - x_0(i)]^2} \quad (4)$$

where MSE is the mean square error, n is the sample size, x_c is the theoretic frequency estimated by marginal distribution or joint function, and x_0 is the empirical frequency for single- or two-dimensional variables estimated by the Gringorten plotting-position formula (Equations (5) and (6)). This formula is expressed as:

$$x_0(i) = P(X \le x_i) = \frac{i - 0.44}{n + 0.12} \quad (5)$$

$$x_0(i) = P(X \le x_i, Y \le y_i) = \frac{\sum_{m=1}^{i}\sum_{l=1}^{i} N_{ml} - 0.44}{n + 0.12} \quad (6)$$

Table 1 | Three common Archimedean copulas in the field of hydrology research

Archimedean copula	$C_\theta(u, v)$	Range	Kendall's tau
Clayton	$(u^{-\theta} + v^{-\theta} - 1)^{-1/\theta}$	$\theta > 0$	$\frac{\theta}{\theta+2}$
Frank	$-\frac{1}{\theta}\ln\left[1 + \frac{(e^{-\theta u} - 1)(e^{-\theta v} - 1)}{e^{-\theta} - 1}\right]$	$\theta \in R$	$1 - \frac{4}{\theta}\left[-\frac{1}{\theta}\int_0^\theta \frac{t}{\exp(t) - 1}dt - 1\right]$
Gumbel–Hougaard	$\exp\left[-\left((-\ln u)^\theta + (-\ln v)^\theta\right)^{1/\theta}\right]$	$\theta \ge 1$	$1 - \frac{1}{\theta}$

where P is the empirical frequency when $X \leq x_i$ (Equation (5)), or $X \leq x_i$ and $Y \leq y_i$ (Equation (6)). i is the ith smallest observation in the dataset arranged in ascending order. $P(X \leq x_i, Y \leq y_i)$ is obtained by arranging (x_i, y_i) by either x_i or y_i, and N_{ml} is the number counted as $x_j \leq x_i$, $y_j \leq y_i$, $i = 1, \ldots, n$, $1 \leq j \leq i$.

Due to the numerous model parameters, the lack-of-fit and unreliability of the model are the two parts of the AIC, which can be expressed as:

$$AIC = -2\ log(maximized\ likelihood\ for\ model) + 2(number\ of\ fitted\ parameters) \quad (7)$$

Additionally, it can be expressed as:

$$AIC = n\ log(MSE) + 2(number\ of\ fitted\ parameters) \quad (8)$$

Thus, the appropriate u and v can be obtained through the two evaluation indices.

Based on the appropriate u and v, the second step is to estimate the parameter θ of the three copula functions by the relationship of the Kendall correlation coefficient τ and the parameter θ (Table 1).

Finally, the joint distribution model is built and the RMSE and AIC indices are again applied to identify the appropriate copula function.

Change point detection based on Archimedean copulas

The joint distribution is defined as:

$$H(x, y) = C_\theta(F(x), G(y)),\ \forall x, y \quad (9)$$

Following Equation (9), the density function can be written as:

$$h(x, y) = f(x)g(y)C_{12}(F(x), G(y)) \quad (10)$$

where $f(x)$ and $g(y)$ represent the density functions and C_{12} can be presented as:

$$C_{12}(u, v) = \frac{\partial}{\partial u}\frac{\partial}{\partial v}C(u, v) \quad (11)$$

The maximum likelihood estimation for the parameters is:

$$\lambda = \arg\max_{\lambda \varepsilon R} \sum_{i=1}^{n} \log C_{12}(\lambda; F(x_i), G(y_i)) \quad (12)$$

Assuming that only one change point exists, the original and alternative hypotheses of the proposition are:

$$H_0: \lambda_1 = \lambda_2 = \ldots = \lambda_n,\ H_1: \lambda_1 = \ldots = \lambda_{k^*} \neq \lambda_{k^*+1} = \ldots = \lambda_n \quad (13)$$

If the original hypothesis is rejected, the change point occurs at the position of k^*. When $k^* = k$, the log likelihood ratio statistic by the maximum likelihood estimation of the joint function can be presented as:

$$-2 \log \wedge_k = 2\left[\begin{array}{l} \sum_{i=1}^{k} \log C_{12}(\lambda_k; F(x_i), G(y_i)) \\ + \sum_{i=k+1}^{n} \log C_{12}(\lambda_{k^*}; F(x_i), G(y_i)) \\ - \sum_{i=1}^{n} \log C_{12}(\lambda_n; F(x_i), G(y_i)) \end{array}\right] \quad (14)$$

where λ_k, λ_{k^*}, and λ_n are the maximum likelihood estimations of parameter λ.

If k^* is unknown and the statistic $Z_n = \max_{1 \leq k \leq n}(-2\log \wedge_k)$ is large, the original hypothesis H_0 can be rejected (i.e., there is a change point) (Ye & Miao 2009). According to the likelihood ratio test methods, the asymptotic distribution of Z_n obeys the $\chi^2(1)$ distribution. The threshold of the Z_n statistic for rejecting the original hypothesis is based on Dias (2004). The time estimation of k^* is shown as:

$$k^* = \arg\max_{1 \leq k \leq n}(-2 \log \wedge_k) \quad (15)$$

The process of change point detection can be briefly summarized as follows:

- Step 1: Select the appropriate marginal distributions for monthly precipitation and runoff.
- Step 2: Estimate the parameter θ of the joint function and establish the joint function for u and v.

- Step 3: Estimate the log likelihood ratio statistic $-2\log\wedge_k$ by Equation (14).
- Step 4: Judge the change point by Equation (15).

If multiple change points exist, the binary segmentation method would be applied to detect the change points between multiple variables. This scenario includes the following: (1) the existence of a single point between the original time series that is detected by the method mentioned above; (2) if no such point exists, the original hypothesis should be accepted; otherwise, the original time series would be divided into two subsequences, and each of them is subject to continued detection; and (3) the process is finished when there is no change point for every subsequence.

Attribution analysis by climate elasticity approach

Runoff change is the consequence of a combination of climate change and human activities, which can be expressed as:

$$\Delta Q = \Delta Q_C + \Delta Q_H \tag{16}$$

$$\Delta Q_C = \Delta Q_P + \Delta Q_{PET} \tag{17}$$

where ΔQ can be obtained by the observation data of a hydrometric station (i.e., $\Delta Q = Q_{obs,2} - Q_{obs,1}$ where $Q_{obs,1}$ and $Q_{obs,2}$ are the runoff before and after the change point, respectively). ΔQ_C and ΔQ_H are the runoff increment induced by climate change and human activities, respectively. ΔQ_P and ΔQ_{PET} are the runoff increments induced by changes in precipitation and PET, respectively. All of these calculations are based on the assumption of mutual independence, which is impacted by climate change and human activities, thus leading to incremental runoff.

The climate elasticity of runoff may be defined as the proportion of the change in runoff (Q) against the change in a climatic variable such as precipitation (P). Thus, precipitation elasticity of runoff is defined as (Liu & Cui 2011):

$$\varepsilon_P(P, Q) = \frac{dQ/Q}{dP/P} = \frac{dQ}{dP}\frac{P}{Q} \tag{18}$$

Based on this, Liu & Cui (2011) have provided estimators to obtain precipitation and PET elasticity of runoff in the Yellow River Basin:

$$\varepsilon_P = \rho_{Q,PET-P}\left(\frac{CV_Q}{CV_P}\right) \tag{19}$$

$$\varepsilon_{PET} = \rho_{Q,P-PET}\left(\frac{CV_Q}{CV_{PET}}\right) \tag{20}$$

where $\rho_{Q,PET-P}$ and $\rho_{Q,P-PET}$ are the partial correlation coefficients of precipitation and PET with runoff, and CV_Q, CV_P, and CV_{PET} are the variation coefficients of runoff, precipitation, and PET, respectively.

Hence, the impact of climate changes and human activities on runoff (ΔQ_C and ΔQ_H, respectively) can be expressed as:

$$\Delta Q_C = \left(\varepsilon_P\frac{\Delta P}{P} + \varepsilon_{PET}\frac{\Delta PET}{PET}\right)Q \tag{21}$$

$$\Delta Q_H = \Delta Q - \Delta Q_C \tag{22}$$

The contribution rates from climate changes and human activities to runoff reduction (C_C and C_H, unit: %) are:

$$C_C = \frac{\Delta Q_C}{\Delta Q}\times 100\% = \frac{\left(\varepsilon_P\frac{\Delta P}{P} + \varepsilon_{PET}\frac{\Delta PET}{PET}\right)Q}{\Delta Q}\times 100\% \tag{23}$$

$$C_H = \frac{\Delta Q_H}{\Delta Q}\times 100\% = \frac{\Delta Q - \Delta Q_C}{\Delta Q}\times 100\% = \left(1 - \frac{\Delta Q_C}{\Delta Q}\right)\times 100\% = 1 - C_C \tag{24}$$

RESULTS

Trends in annual hydro-meteorological variables

Long-term variations of annual runoff, precipitation, and PET in the WRB from 1960 to 2010 show decreases in annual runoff and precipitation and an increase in annual PET (Figure 2). The results of the nonparametric Mann–Kendall (MK) trend test show that annual runoff (MK value −3.79) presents a significant decreasing trend at the 95% significance level

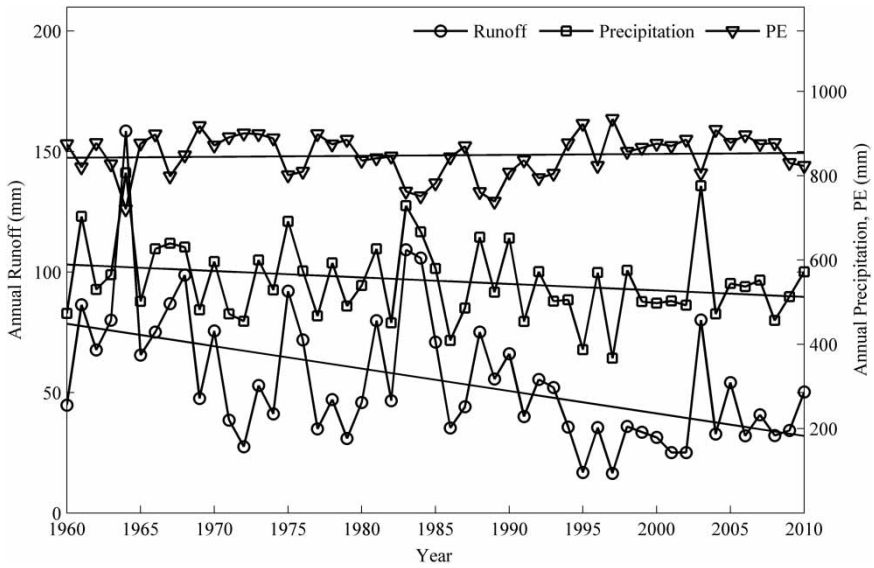

Figure 2 | Annual runoff, precipitation, and PET changes in 1960–2010 in the WRB.

during the period of 1960–2010, while annual precipitation (MK value −1.63) presents a decreasing but insignificant trend. The annual PET presents an increasing trend but fails to pass the significance test at the 95% significance level.

The MK trend test results for monthly precipitation, runoff, and PET are all negative for monthly runoff from 1960 to 2010, which indicates that monthly runoff shows a decreasing trend (Figure 3). The MK values for runoff in January, February, June, August, and December are all larger than the critical value of −1.96 at the 95% significance level, indicating that the runoff in these months exhibits a decreasing but insignificant trend. Runoff in the remaining months exhibits a decreasing and significant trend with MK values less than the critical value of −1.96 at the 95% significance level.

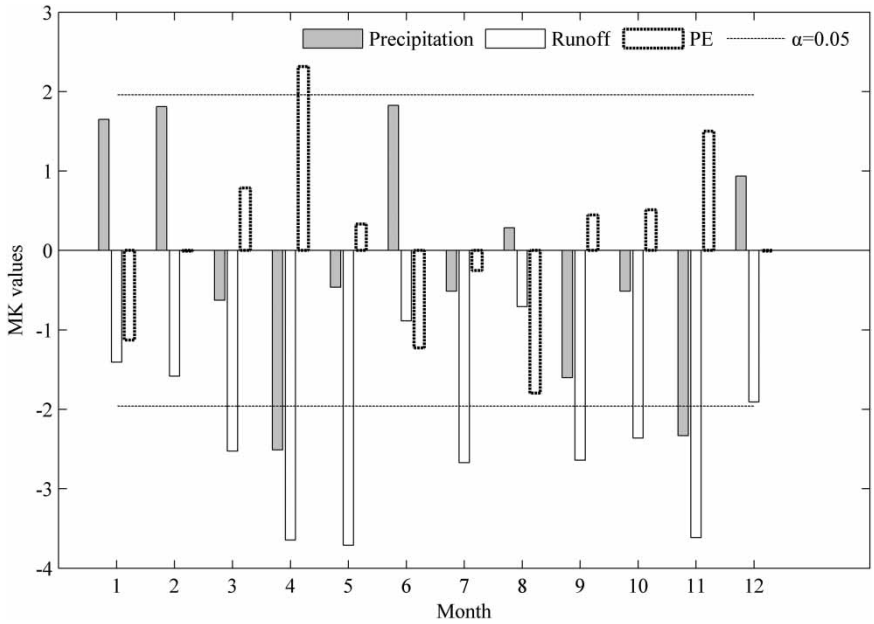

Figure 3 | The MK test results of monthly precipitation, runoff, and PET in 1960–2010 in the WRB. The horizontal dashed lines represent the critical value of the 95% significance level.

For monthly precipitation, there is an insignificant upward trend in January, February, June, August, and December; however, precipitation in the remaining months presents a downward trend. In particular, precipitation in April and November has a significant downward trend at the 95% significance level. Although annual PET is increasing, the PET in January, June, July, and August decreases but is not statistically significant. The PET in April showed a statistically significant upward trend from 1960 to 2010.

Detection of PRR change points

Selection of the appropriate marginal distribution

As introduced in the section 'Change point detection based on Archimedean copulas', the Gev, Logn, and Gam distributions were used to fit monthly precipitation and runoff with little difference among the three marginal distributions (Figure 4). To obtain a better marginal distribution, the RMSE and AIC for monthly runoff and precipitation were calculated and are listed in Table 2. It can be easily seen from Table 2 that the Gam and Logn distributions are the more appropriate marginal distributions because of the smaller RMSE and AIC.

Selection of the appropriate copula function

The frequency obtained by the joint distribution model shows that the correlation coefficients of the Clayton, Frank, and Gumbel–Hougaard copula-based calculation probability distributions, and the empirical probability distributions are both above 0.99 (Figure 5). Thus, there is little difference between the three joint functions modeling monthly runoff and precipitation.

Therefore, the RMSE and AIC were again applied to select the appropriate joint distribution model, and as a result, the Gumbel–Hougaard copula was chosen (Table 3).

Change point detection

Zn was calculated by Equations (14) and (15), and shows that there may be two turning points occurring in 1971 and 1994 (Figure 6). Therefore, the binary segmentation method was applied to further study the PRR change point, and the results are shown in Figure 6(b) and 6(c). It can be inferred from Figure 6 that the change points of PRR occurred in 1971 and 1994, with a *Zn* value beyond the critical value of 9.

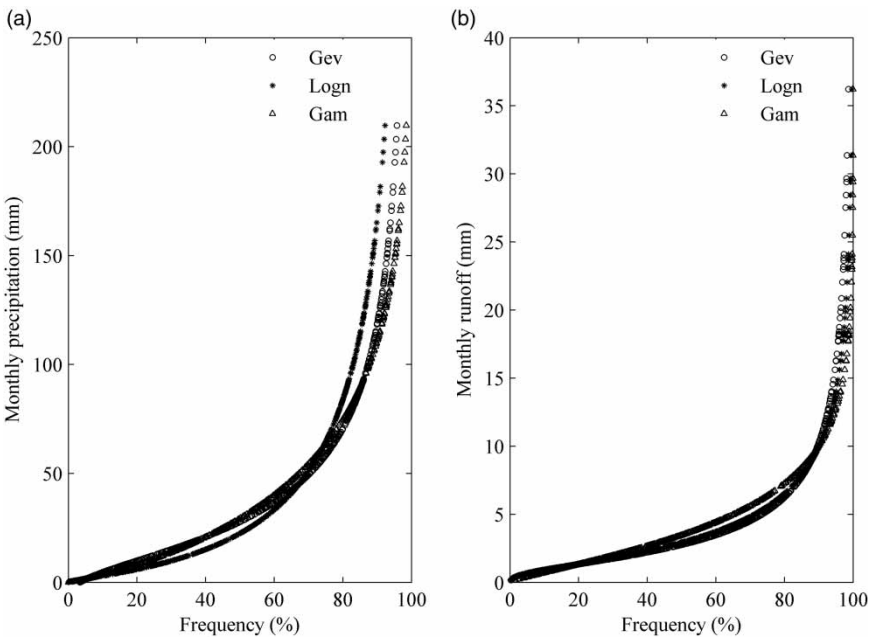

Figure 4 | Monthly precipitation (a) and runoff (b) frequency curves on different marginal distributions.

Table 2 | Fitted effect of different marginal distributions on monthly precipitation and runoff in the WRB

Hydrological variables	Model of marginal distribution	RMSE	AIC
Monthly precipitation	Gev	0.048	−1611.35
	Logn	0.061	−1485.58
	Gam	0.028	−1906.21
Monthly runoff	Gev	0.018	−2138.10
	Logn	0.012	−2342.58
	Gam	0.047	−1625.78

DISCUSSION

Comparative analysis of the PRR change point

The change point detection results of PRR in this paper are similar to the results of Su *et al.* (2007), Hou *et al.* (2011), and Bi *et al.* (2013) using the double mass curve method in the WRB. Su *et al.* (2007) proved the PRR change point of 1971 while failing to obtain the other change points. Bi *et al.* (2013) only detected a single change point in 1994. Hou *et al.* (2011) found PRR change points occurring in 1971, 1983, 1994, and 2003. We also applied the double mass curve method in the WRB and were unable to accurately judge PRR change points, showing that the validity of this method is limited in the WRB (Figure 7).

The judgment of PRR change point(s) is clearly subjective and displays uncertainties (Figure 7). In contrast, determination of the change point(s) by the method based on the Archimedean copulas is accurate and reliable.

Change in PRR

Time series of precipitation and runoff were divided into three stages separated by the change points in 1971 and 1994, representing natural (1960–1971) and impacted periods (1972–1994 and 1995–2010). The PRR is the lowest from 1995 to 2010, followed by 1972–1994 and then 1960–1971; this implies that runoff yield increased from 1995–2010 to 1972–1994 to 1960–1971 at the same annual precipitation (Figure 8).

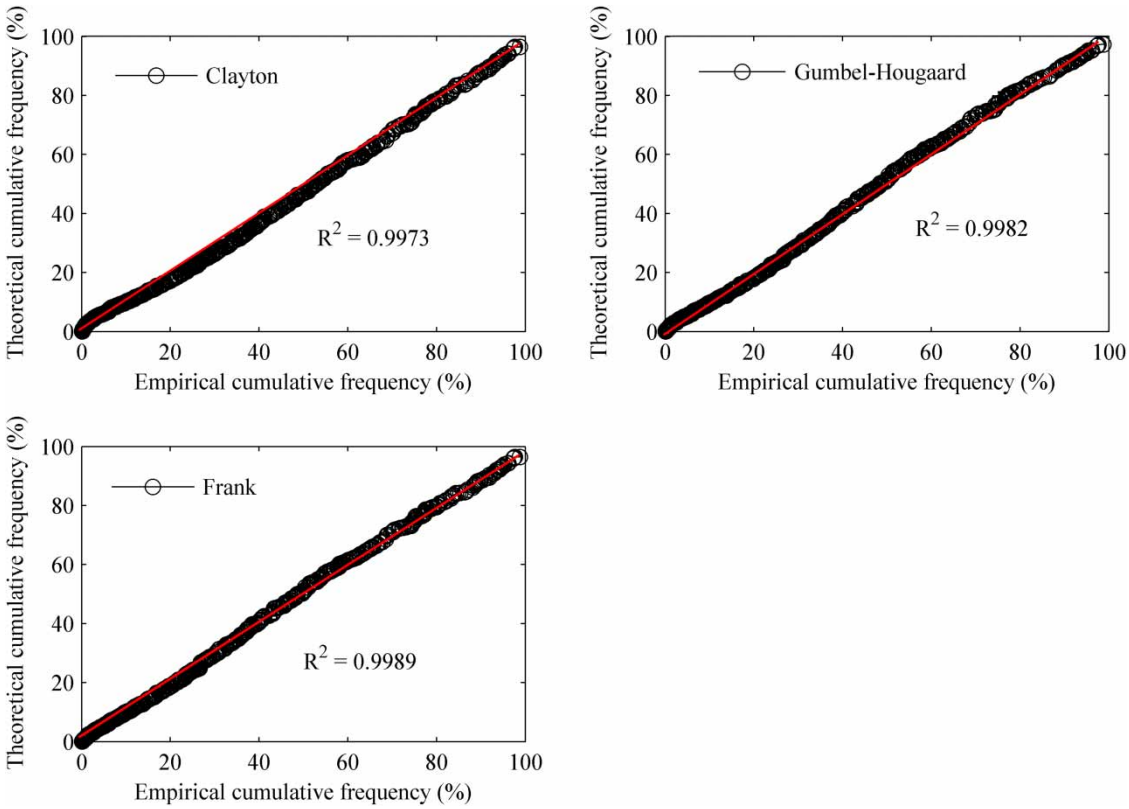

Figure 5 | Comparisons of theoretical cumulative frequency obtained by Archimedean copulas with empirical cumulative frequency.

Table 3 | The goodness-of-fit test of Archimedean copulas

Joint function	RMSE	AIC
Clayton copula	0.43	−443.32
Frank copula	0.44	−440.03
Gumbel–Hougaard copula	0.42	−458.14

For example, when annual precipitation was 600 mm, annual runoff yields were approximately 74, 63, and 46 mm, respectively, during 1960–1971, 1972–1994, and 1995–2010. The linear regression rates of runoff to precipitation for the three periods are 0.28, 0.23, and 0.15, indicating that runoff increased more pre-1971 than in the post-1994 period with the same change in annual precipitation.

Change in precipitation and runoff before and after the change points of PRR

Annual and intra-annual changes in precipitation and runoff

Several indices show that mean annual runoff in the periods of 1972–1994 and 1995–2010 was 57.25 and 36.03 mm, or 25.78% and 53.29% lower than the 1960–1971 period, respectively (Table 4). By contrast, the precipitation change was smaller, with reductions of 5.32% and 11.23% for the 1972–1994 and 1995–2010 periods, respectively. The variation coefficients of inter-annual (Inter-Cv) runoff and precipitation were not significantly altered, although the inter-annual variability of runoff was higher than that of precipitation. Based on the concentration degree (CD) (Zhang & Qian 2003) and intra-annual variation coefficients (Intra-Cv), there is little change in precipitation but a more obvious change in runoff.

The precipitation in September shows the most dramatic change throughout the three different periods (Figure 9). Maximum runoff occurred in September, September, and October for the 1960–1971, 1972–1994, and 1995–2010 periods, respectively, and the intra-annual change is more uniform in 1995–2010 than either of the previous periods.

Changes in precipitation and runoff characteristics

Duration curves constructed with monthly runoff and precipitation in different periods in the WRB can visualize

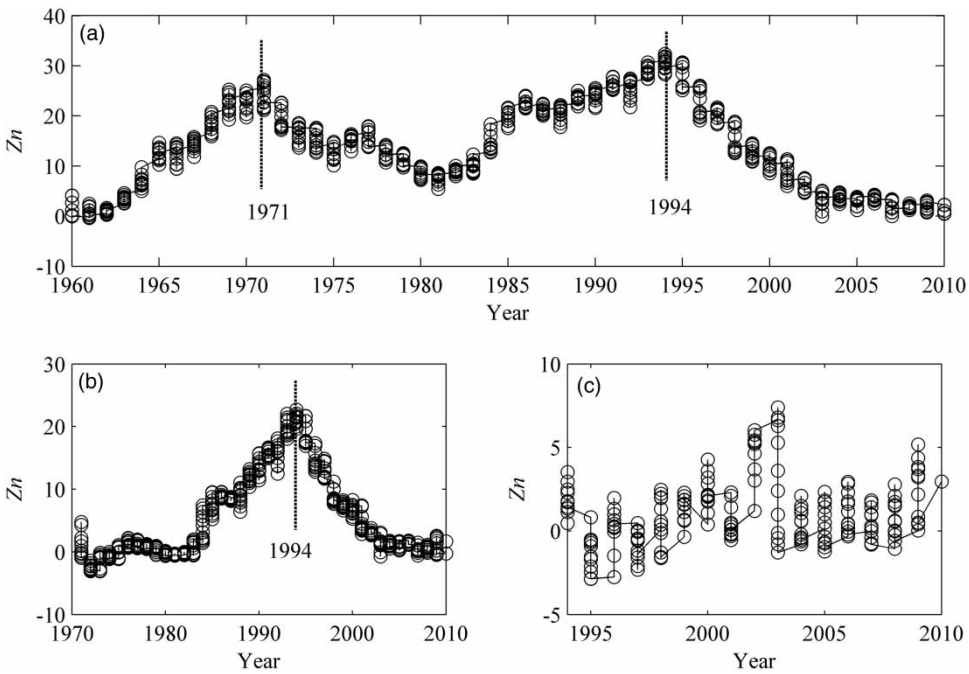

Figure 6 | Changes of statistics *Zn* estimated by Equation (14) and the dashed lines represent the occurrence time of change point of PRR.

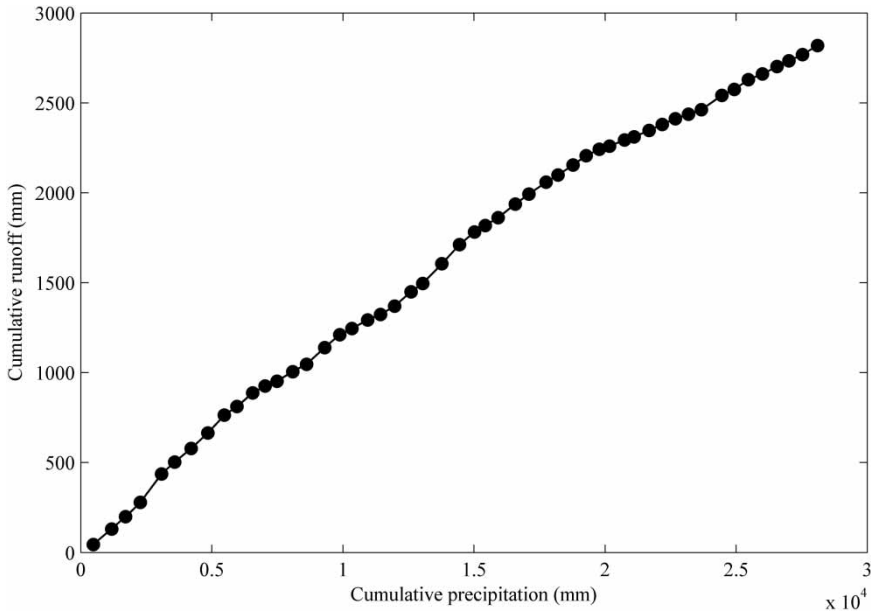

Figure 7 | Double mass curve of annual precipitation and runoff for 1960–2010 in the WRB.

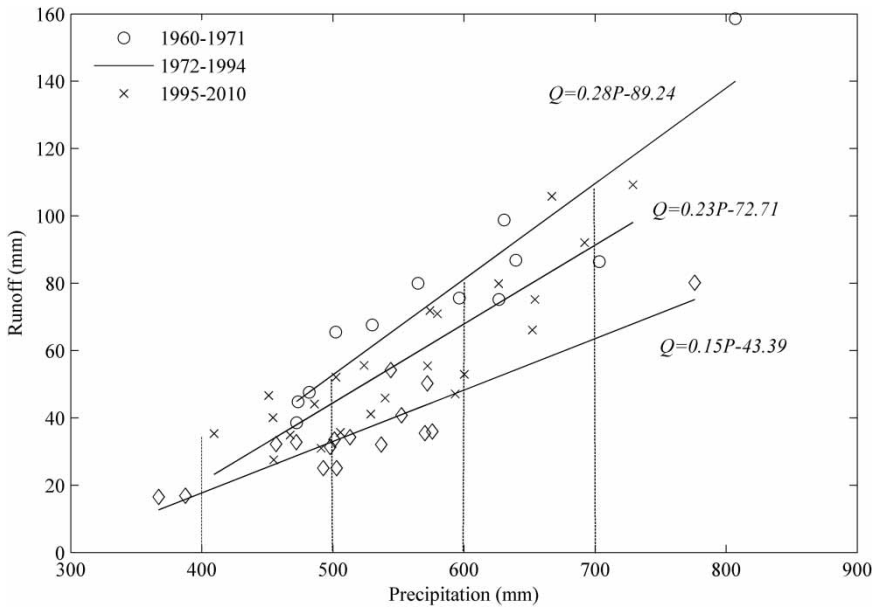

Figure 8 | PRR for three periods, 1960–1971, 1972–1994, and 1995–2010 in the WRB.

the impacts of rainfall pattern, catchment size, land use, and river engineering through the change in duration curves (Figure 10 and Table 5). The change in monthly runoff declined more than precipitation at various frequencies in different periods in the WRB.

Compared with the duration curve of the 1960–1971 period, the most remarkable change in monthly runoff duration curves occurs at the 95% exceedance probability in 1972–1994. Here, the curve declines by 42.02%, while precipitation increases by 28.71%. Runoff at the 50% and 5%

Table 4 | Changes of characteristics of runoff and precipitation in 1960–1971, 1972–1994, and 1995–2010 in the WRB

	Runoff			Precipitation		
Index	1960–1971	1972–1994	1995–2010	1960–1971	1972–1994	1995–2010
Average (mm)	77.13	57.25	36.03	585.64	554.49	519.86
Inter-Cv	0.41	0.40	0.43	0.18	0.16	0.18
CD (%)	28	32	34	35	35	36
Intra-Cv	0.78	0.90	0.83	0.94	0.94	0.96

exceedance probabilities declined by 30.62% and 13.83% compared with precipitation, which declined by 25.20% and 8.98%, respectively.

Compared with the duration curve for the 1960–1971 period, runoff in 1995–2010 decreased by 53% and 50% for the 5% and 95% exceedance probabilities, respectively; these changes are more significant than the change in precipitation (−13.63%, −33.72%, and 66.34%, respectively).

What is responsible for the change in PRR?

The correlation between precipitation and runoff decreased for the 1972–1994 and 1995–2010 periods compared to the 1960–1971 period, and annual runoff yield significantly decreased at the same annual precipitation. Compared with runoff and precipitation from 1960 to 1971, the mean annual runoff declined by 25.78% and 53.29% in 1972–1994 and 1995–2010, respectively, whereas mean annual precipitation declined by only 5.32% and 11.23%, respectively. Although the change in monthly runoff is notable, there was little change in monthly precipitation. The asynchronous changes in precipitation and runoff may be the driving force behind the changes in PRR. Due to the minimal changes in precipitation, it is essential to determine the reason for the changes in runoff. To this end, the climate elasticity of runoff method (Liu & Cui 2011) was applied to study the impact of climate changes (i.e., precipitation and PET) and human activities on runoff reduction (Table 6).

Human activities are the dominant factors (84.15%) leading to decreases in runoff for the periods of 1972–1994 and 1995–2010 (84.15% and 57.16%, respectively). Du & Shi

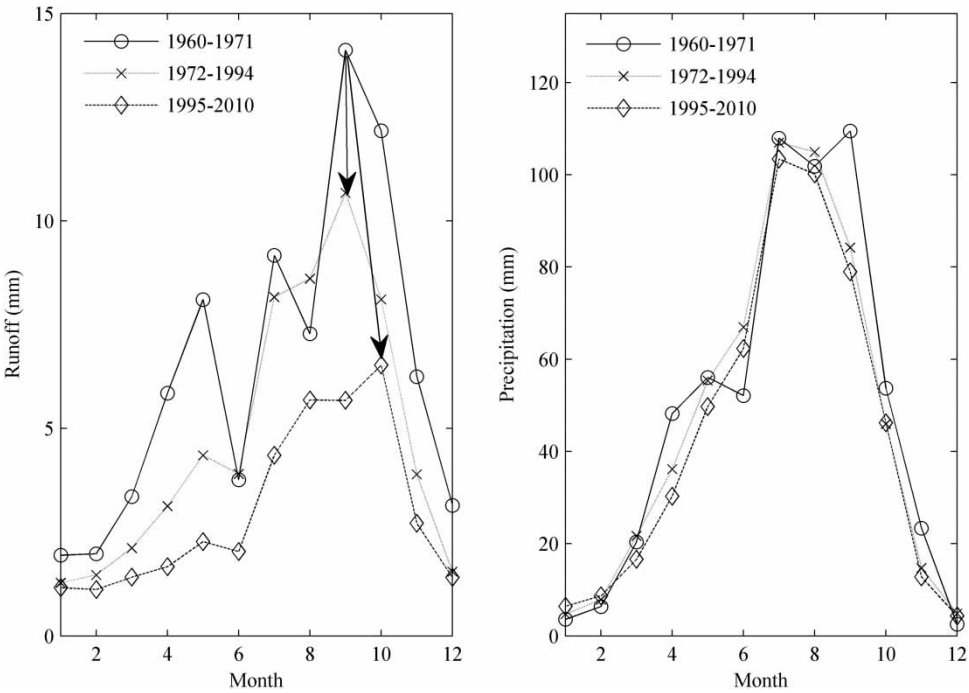

Figure 9 | Monthly runoff and precipitation changes in different periods in the WRB.

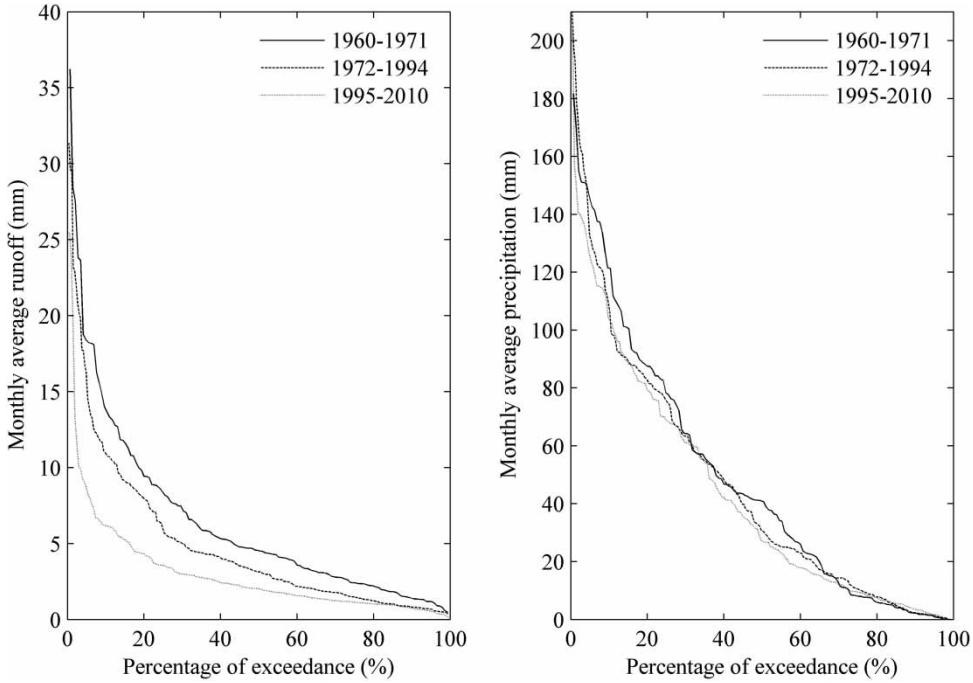

Figure 10 | Duration curves of monthly runoff and precipitation in different periods in the WRB.

Table 5 | Characteristics of monthly runoff and precipitation from Figure 10 in different periods in the WRB

		Exceedance probabilities		
Elements	**Characteristic values**	**5%**	**50%**	**95%**
Runoff	$R_{(1960–1971)}$	18.37 mm	4.54 mm	1.19 mm
	$R_{(1972–1994)}$	15.83 mm	3.15 mm	0.69 mm
	$R_{(1995–2010)}$	8.62 mm	2.03 mm	0.55 mm
	Change ratio (1972–1994 versus 1960–1971)	−13.83%	−30.62%	−42.02%
	Change ratio (1995–2010 versus 1960–1971)	−53.08%	−55.29%	−53.78%
Precipitation	$P_{(1960–1971)}$	145.39 mm	40.95 mm	1.01 mm
	$P_{(1972–1994)}$	132.34 mm	30.63 mm	1.30 mm
	$P_{(1995–2010)}$	125.57 mm	27.14 mm	1.68 mm
	Change ratio (1972–1994 versus 1960–1971)	−8.98%	−25.20%	28.71%
	Change ratio (1995–2010 versus 1960–1971)	−13.63%	−33.72%	66.34%

Table 6 | Impacts of climate variability and human activities on runoff reduction by climate elasticity of runoff method in the WRB

				Climate change		Human activities	
Periods	**Runoff (mm)**	**Precipitation (mm)**	**PET (mm)**	**ΔQ_C (mm)**	**C_C**	**ΔQ_H (mm)**	**C_H**
1960–1971	77.13	585.64	851.68				
1972–1994	57.25	554.49	830.69	−3.15	15.85%	−16.73	84.15%
1995–2010	36.03	519.86	870.47	−17.61	42.84%	−23.49	57.16%

(2012) used the measured and natural runoff in the WRB to determine that human activities accounted for 51.11% of the runoff reduction in 1988–2008 compared to 1956–1987, while climate change accounted for 48.49%. Zhan *et al.* (2014) combined an elasticity coefficient approach and hydrological model (SIMHYD model) to conclude that the contributions of climate change and human activities to runoff change in 1990–2008 compared with 1958–1989 were 34.1 ~ 47.3% and 52.7 ~ 65.9%, respectively. Chang *et al.* (2015) used the variable infiltration capacity hydrological model and found that the contribution to runoff changes for the 1970s, 1980s, 1990s, and 2000s from climate change were 36%, 28%, 53%, and 10%, respectively, and 64%, 72%, 47%, and 90%, respectively, from human activities. The results of our study are similar in that human activities were the main factor driving the decrease in runoff in the WRB. Additionally, the contribution of climate changes to the runoff decrease was enhanced in the 1990s. These results show that human activities are the dominant factor influencing the change in PRR. Irrigated areas, water projects, and water and soil conservation are direct causes of the runoff change in the WRB (Du & Shi 2012; Chang *et al.* 2015).

In the study area, use of the Baojixia (1,948 km^2), Jinghuiqu (894 km^2), and Fengjiashan (909 km^2) irrigation areas has increased gradually since the 1970s, and the large amount of water discharged by irrigation fields has directly resulted in decreased runoff. For example, in the Baojixia irrigation area, the diverted water volume can reach up to 0.60 billion m^3 per year (Bi *et al.* 2013). By the end of 2000, there had been 302 large, medium, and small-scale reservoirs constructed, with a total storage capacity of 2.73 billion m^3; these are used primarily for irrigation and industry (Figure 11). Excess reservoirs were constructed in the period of 1970–1975, and these projects have led to the redistribution of inter- and intra-annual runoff in the WRB.

To control water and soil loss, soil conservation projects, such as afforestation, grass-planting, and construction of level terraces and check dams have been implemented in the study area beginning in the 1970s. Zhao *et al.* (2001) used the soil hydrology method to calculate the effect of water reduction from soil and water conservation. They showed that the mean annual water reduction was 2.85 billion m^3 from 1990 to 1996, and was mainly caused by human activities and precipitation (51.5% and 48.5%, respectively).

Yao *et al.* (2011) found that the El Nino event that occurred in 1994 also resulted in a significant drop in precipitation. After 1994, there were fewer soil and water conservation projects in the WRB, and climate change was

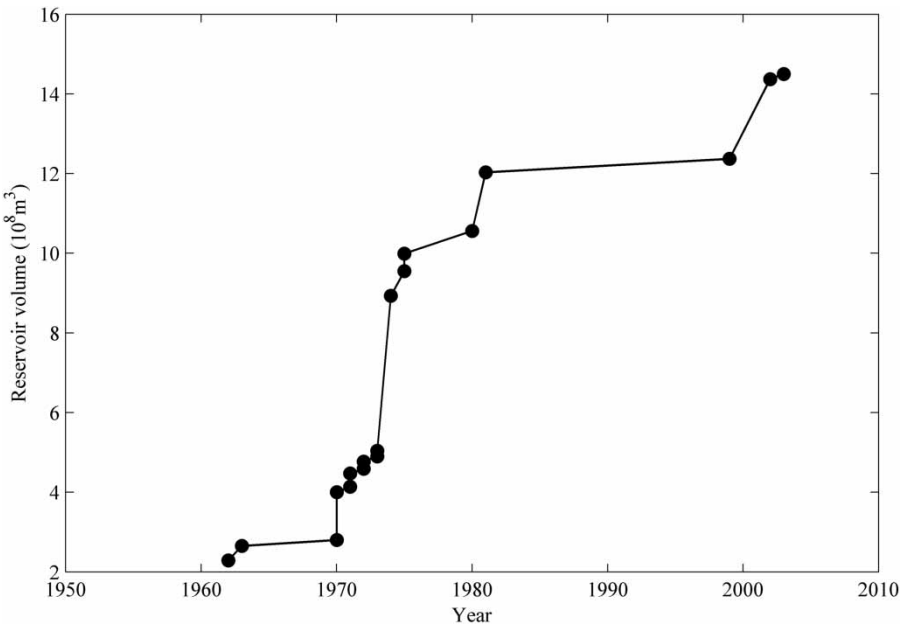

Figure 11 | Changes of reservoir (large- and middle-sized reservoirs) volumes in the WRB of Shaanxi province for 1960–2010.

more notable than before. Thus, the role of climate change on runoff is greater than ever.

CONCLUSIONS

Based on monthly runoff and precipitation from 1960 to 2010, the change in PRR was studied using the Archimedean copulas. We identified the change points in the PRR relationship and identified the driving forces behind the change points. The following conclusions were drawn:

1. Some of the decreasing trends in annual runoff and precipitation were significant at the 95% significance level by the MK trend test, and others were not; however, there were minimal changes in annual PET. In the WRB, the change points in the PRR occurred in 1971 and 1994; these dates were used to divide the whole time series into three periods: 1960–1971, 1971–1994, and 1995–2010.
2. The runoff yield was the highest in 1960–1971, followed by 1972–1994, and then 1995–2010 under the same annual precipitation. The inter-annual and intra-annual variations in precipitation were less obvious than for runoff. Comparing the duration curves of different periods showed that the change in monthly runoff declined more than precipitation at various exceedance probabilities. Therefore, it was concluded that the change in PRR was primarily caused by a decline in runoff due to human activities in the WRB.
3. Irrigated areas, water projects, and water and soil conservation efforts directly contributed to changes in runoff in the WRB. Compared with runoff in 1960–1971, human activities account for 84.15% and 57.16% of the runoff reduction in 1972–1994 and 1995–2010, respectively, while climate changes account for 15.85% and 42.84%. It is clear that human activities have played a more dominant role in changing the PRR than climate change.

ACKNOWLEDGEMENTS

This research was supported by the Natural Science Foundation of China (51190093) and Key Innovation Group of Science and Technology of Shaanxi (2012KCT-10). Sincere gratitude is extended to the editor and the anonymous reviewers for their professional comments and corrections.

REFERENCES

Allen, R. G., Pereira, L. S., Raes, D. & Smith, M. 1998 *Crop evapotranspiration: Guidelines for computing crop water requirements*. FAO Irrigation and Drainage Paper 56. Food and Agriculture Organization of the United Nations (FAO), Rome, Italy.

Areerachakul, S. & Junsawang, P. 2014 Rainfall-runoff relationship for streamflow discharge forecasting by ANN modelling. In: *2014 World Congress on Sustainable Technologies*, 8–10 December, London, UK, pp. 27–30.

Bi, C. X., Mu, X. M., Zhao, G. J. & Bai, H. 2013 Effects of climate change and human activity on streamflow in the Wei River Basin. *Sci. Soil Water Conserv.* **11**, 33–38 (in Chinese).

Chang, J. X., Wang, Y. M., Istanbulluoglu, E., Bai, T., Huang, Q., Yang, D. W. & Huang, S. Z. 2015 Impact of climate change and human activities on runoff in the Weihe River Basin, China. *Quatern. Int.* **380–381**, 169–179.

Charlier, J. B., Ladouche, B. & Maréchal, J. C. 2015 Identifying the impact of climate and anthropic pressures on karst aquifers using wavelet analysis. *J. Hydrol.* **523**, 610–623.

Dias, A. 2004 Copula inference for finance and insurance. *Doctoral thesis*, ETH No. 15283, Swiss Federal Institute of Technology, Zurich, Switzerland.

Du, J. & Shi, C. X. 2012 Effects of climatic factors and human activities on runoff of the Weihe River in recent decades. *Quatern. Int.* **282**, 58–65.

Faisal, N. & Gaffar, A. 2012 Development of Pakistan's new area weighted rainfall using Thiessen polygon method. *Pakistan J. Meteorol.* **9**, 107–116.

Genest, C. & MacKay, J. 1986 The joy of copulas: bivariate distributions with uniform marginals. *Am. Stat.* **40** (4), 280–283.

Hou, Q. L., Bai, H. Y., Ren, Y. Y., He, Y. N. & Ma, X. P. 2011 Analysis of variation in runoff of the main stream of the Weihe River and related driving forces over the last 50 years. *Res. Sci.* **33**, 1505–1512 (in Chinese).

Huang, S. Z., Huang, Q., Chang, J. X., Chen, Y. T., Xing, L. & Xie, Y. Y. 2015 Copulas-based drought evolution characteristics and risk evaluation in a typical arid and semi-arid region. *Water Resour. Manage.* **29**, 1489–1503.

Jiang, C., Xiong, L. H., Xu, C. Y. & Guo, S. L. 2015a Bivariate frequency analysis of nonstationary low-flow series based on the time-varying copula. *Hydrol. Process.* **29**, 1521–1534.

Jiang, C., Xiong, L. H., Wang, D. B., Liu, P., Guo, S. L. & Xu, C. Y. 2015b Separating the impacts of climate change and human activities on runoff using the Budyko-type equations with time-varying parameters. *J. Hydrol.* **522**, 326–338.

Labat, D., Ababou, R. & Mangin, A. 2001 Introduction of wavelet analyses to rainfall-runoffs relationship for karstic basins: the case of Licq-Atherey karstic system (France). *Ground Water* **39** (4), 605–615.

Liu, Q. & Cui, B. S. 2011 Impacts of climate change/variability on the streamflow in the Yellow River Basin, China. *Ecol. Model.* **222**, 268–274.

Mwale, D., Gan, T. Y., Devito, K., Mendoza, C., Silins, U. & Petrone, R. 2009 Precipitation variability and its relationship to hydrologic variability in Alberta. *Hydrol. Process.* **23**, 3040–3056.

Nourani, V., Khanghah, T. R. & Baghanam, A. H. 2015 Application of entropy concept for input selection of wavelet-ANN based rainfall-runoff modeling. *J. Environ. Inform.* **26**, 52–70.

Partal, T. 2012 Wavelet analysis and multi-scale characteristics of the runoff and precipitation series of the Aegean region (Turkey). *Int. J. Climatol.* **32**, 108–120.

Rahmani, M. A. & Zarghami, M. 2015 The use of statistical weather generator, hybrid data driven and system dynamics models for water resources management under climate change. *J. Environ. Inform.* **25**, 23–35.

Rege, S., Arenz, M., Marvuglia, A., Vázquez-Rowe, I., Benetto, E., Igos, E. & Koster, D. 2015 Quantification of agricultural land use changes in consequential life cycle assessment using mathematical programming models following a partial equilibrium approach. *J. Environ. Inform.* **26**, 121–139.

Searcy, J. K., Hardisoni, C. H. & Langbein, W. B. 1960 *Double mass curves*. Geological Survey Water Supply Paper 1541-B, US Geological Survey, Washington, DC, USA.

Su, X. L., Kang, S. Z., Wei, X. M., Xing, D. W. & Cao, H. X. 2007 Impact of climate change and human activity on the runoff of Wei River basin to the Yellow River. *J. Northwest Sci-Tech. Univ. Agric. For. (Nat. Sci. Ed.).* **35**, 153–159 (in Chinese).

Velpuri, N. M. & Senay, G. B. 2013 Analysis of long-term trends (1950–2009) in precipitation, runoff and runoff coefficient in major urban watersheds in the United States. *Environ Res. Lett.* **8**, 279–288.

Wang, F., Hessel, R., Mu, X. M., Maroulis, J., Zhao, G. J., Geissen, V. & Ritsema, C. 2015 Distinguishing the impacts of human activities and climate variability on runoff and sediment load change based on paired periods with similar weather conditions: a case in the Yan River, China. *J. Hydrol.* **527**, 884–893.

Xiong, L. H., Jiang, C. & Du, T. 2014 Statistical attribution analysis of the nonstationarity of the annual runoff series of the Weihe River. *Water. Sci. Technol.* **70** (5), 939–946.

Yang, Y. H. & Tian, F. 2009 Abrupt change of runoff and its major driving factors in Haihe river catchment, China. *J. Hydrol.* **374**, 373–383.

Yao, Y. B., Zhang, X. Y. & Duan, Z. Y. 2011 Climate evolution and its impact to water resource changer in source of Wei river basin. *Agricultural Research in the Arid Areas* **29** (5), 247–252 (in Chinese).

Ye, W. Y. & Miao, B. Q. 2009 Analysis of sub-prime loan crisis contagion based on change point testing method of copula. *Chinese J. Manage. Sci.* **17**, 1–7 (in Chinese).

Zhan, C. S., Zeng, S. D., Jiang, S. S., Wang, H. X. & Ye, W. 2014 An integrated approach for partitioning the effect of climate change and human activities on surface runoff. *Water Resour. Manage.* **28**, 3843–3858.

Zhang, L. J. & Qian, Y. F. 2003 Annual distribution features of the yearly precipitation in China and their inter annual variations. *Acta Meteorol. Sin.* **17**, 146–163.

Zhang, Z. X., Chen, X., Xu, C. Y., Yuan, L. F., Yong, B. & Yan, S. F. 2011 Evaluating the non-stationary relationship between precipitation and streamflow in nine major basins of China during the past 50 years. *J. Hydrol.* **409**, 81–93.

Zhao, J. X., Wang, H., Ma, Y. & Yan, G. L. 2001 Preliminary analysis on cause of water and sediment variation from 1990–1996 in Weihe watershed. *J. Soil Water Conserv.* **15**, 136–139 (in Chinese).

Zuo, D. P., Xu, Z. X., Yang, H. & Liu, X. C. 2012 Spatiotemporal variations and abrupt changes of potential evapotranspiration and its sensitivity to key meteorological variables in the Wei River basin, China. *Hydrol. Process.* **26**, 1149–1160.

First received 15 January 2016; accepted in revised form 1 March 2016. Available online 4 April 2016